Dust acoustic waves in three-dimensional complex plasmas with a similarity property

D. I. Zhukhovitskii*

Joint Institute of High Temperatures, Russian Academy of Sciences, Izhorskaya 13, Bd. 2, 125412 Moscow, Russia

(Received 29 June 2015; published 28 August 2015)

Dust acoustic waves in the bulk of a dust cloud in complex plasma of low-pressure gas discharge under microgravity conditions are considered. The complex plasma is assumed to conform to the ionization equation of state (IEOS) developed in our previous study. This equation implies the ionization similarity of plasmas. We find singular points of IEOS that determine the behavior of the sound velocity in different regions of the cloud. The fluid approach is utilized to deduce the wave equation that includes the neutral drag term. It is shown that the sound velocity is fully defined by the particle compressibility, which is calculated on the basis of the used IEOS. The sound velocities and damping rates calculated for different three-dimensional complex plasmas both in ac and dc discharges demonstrate a good correlation with experimental data that are within the limits of validity of the theory. The theory provides interpretation for the observed independence of the sound velocity on the coordinate and for a weak dependence on the particle diameter and gas pressure. Predictive estimates are made for the ongoing PK-4 experiment.

DOI: 10.1103/PhysRevE.92.023108 PACS number(s): 52.27.Lw, 52.35.Fp, 82.70.−y

I. INTRODUCTION

A low-temperature plasma, which includes dust particles with sizes ranging from 1 to 10^3 μm, is usually referred to as dusty or complex plasma. Since the mobility of electrons is much greater than that of ions, particles acquire a significant negative electric charge. This leads to formation of a strongly coupled plasma [1–9], in which various collective phenomena at the level of individual particles can be observed. Complex plasmas are studied in gas discharges at low pressures, e.g., in radio frequency (RF) discharges. Under microgravity conditions, large volumes of three-dimensional (3D) complex plasma can be observed. These conditions are realized either in parabolic flights [10–14] or on board the International Space Station (ISS) [10,15–20].

The PK-4 project is intended to be a continuation of successful series of PK-1, PK-2, PK-3, and PK-3 Plus experiments on board the ISS. The PK-4 setup was exhaustively tested in ground-based conditions [21] and in parabolic flights [22–24]. Since the PK-4 experiments are focused on dynamical phenomena in complex plasmas including formation and propagation of the shock waves and solitons, investigation of the waves associated with the motion of dust particles is of special interest. The linear waves with a long wavelength larger than the interparticle distance and the Debye length are commonly called dust acoustic waves (DAWs).

From the time that the notion of DAWs was first introduced by Rao, Shukla, and Yu [25], DAWs became a subject of extensive investigations [26]. Havnes *et al.* [27] predicted that if the disturbance generating DAWs in a strongly coupled system of the dust particles moves with a supersonic velocity, then the Mach cone emerges. The Mach cone observations were used for the determination of dust sound velocity, first, in the experiments with a 2D lattice plane [28–34] and then in a 3D strongly coupled system of charged particles [11,12,14,19,20] formed in RF discharge in argon. In Ref. [35], the Mach cone observation in a complex plasma of the neon RF discharge was used for the determination of the dust sound velocity. An interesting feature of the 3D studies was independence of the sound velocity (within the experimental error) of the system parameters such as the dust particle radius, argon pressure, and the location in the bulk of a dust cloud. The latter fact is most surprising because according to the assessment [36], the particle number density in the inner and outer regions of the dust cloud differ almost by an order of magnitude; the particle charge also changes significantly along the bulk of the cloud. In addition, the sound velocity was found to be isotropic; i.e., it is independent of the direction of wave propagation with respect to the direction of the gas discharge electric field. In experiments with argon [11,12,14,19,20], the measured sound velocity ranged from 2 to 3 cm/s; the sound velocity measured in neon proved to be twice as low (about 1 cm/s) [35], but it was still independent of the particle number density.

In the pioneer work [25], calculation of the dust sound velocity was based on the fluid approach. This result is valid if the dust component of the complex plasma conforms to the ideal gas equation of state while the average kinetic energy of particles (particle temperature T_d) is equal to zero. The resulting formula for the sound velocity is similar to that for the ion acoustic waves [37]. However, the systems of dust particles, for which the sound velocity was measured, are strongly coupled with a typical coupling parameter $\Gamma = Z^2e^2/r_dT_d > 200$ [38], where Z is the dust particle charge in units of the electron charge, e is the elementary electric charge, $r_d = (3/4\pi n_d)^{1/3}$ is the Wigner–Seitz radius for the dust particles, n_d is the particle number density, and the Boltzmann constant is set to unity. Note that this estimate is most likely a low bound for Γ, which relates to the smallest particles used in experiments and to the lowest estimates for the particle charge; for real systems, Γ can be orders of magnitude higher. Note that the dust kinetic temperature determined experimentally is rather high: according to Ref. [39], $T_d < 0.8$ eV; in Ref. [40], the dust temperature was found to be in the range from 0.1 to 1 eV. Thus, $T_d/T_n \sim 30$, where T_n is the temperature of gas molecules usually assumed to be equal to room temperature. In spite of this fact, $\Gamma \gg 1$.

*dmr@ihed.ras.ru

Khrapak and Thomas [41] showed that for strongly coupled Yukawa systems, the dust sound propagation is defined by the nonzero compressibility of the particles resulting from their correlation energy. The term in the expression for the sound velocity corresponding to the electric field perturbation due to charge separation in the sound wave, which was solely taken into account in Ref. [25], appeared to be canceled out exactly by the plasma-related contribution to the isothermal compressibility modulus. However, the results of this work are not directly applicable to the complex plasmas because the latter is different from the Yukawa systems [42,43]. A principal difference comes from the fact that the complex plasma is an open system characterized by an intense energy exchange with the environment; due to the production of electrons and ions, their recombination and loss on chamber walls, and charging of the dust particles, the charged components of complex plasma do not form a fixed ensemble. Therefore, equilibrium thermodynamics along with all related thermodynamic notions such as the entropy *is not applicable* for this system. Another difference lies in the presence of an external electric field typical for both the ac and dc discharges. This field is responsible for the emergence of ion drag force, which along with the electric field defines the dynamics of dust particles [36]. It is also important that the particle charge is not fixed but is a function of the local number densities of electrons, ions, and particles, whose variation may reach an order of magnitude. Note that the particle charge variation was not allowed for in Refs. [25] and [41]. Nevertheless, the real complex plasma can be *locally* treated as a system of strongly correlated particles on a uniform charge background formed by the electrons and ions, i.e., as the one-component plasma. This determines a principal similarity between the complex plasma and the strongly coupled Yukawa system.

The objective of this work is to develop a theory of DAWs propagation in a real system (the dust cloud in a low-pressure discharge). Our approach is based on the model of complex plasma [36]. According to this model, the dust cloud can be stable if the electric force from an external electric field is balanced by the force due to collisions with the ions drifting in this electric field (ion drag force). The key assumption of the model is overlapping of the Coulomb potentials of neighboring particles, due to which the cross section of ion scattering on the particles is a function of the particle number density. This made it possible to relate the number density of electrons, ions, and particles and the particle charge in such a way that each parameter defines uniquely the others. The "dust invariant" was obtained that is nearly constant for the dust clouds observed in different experiments. As a consequence, a reasonable estimation for the stationary particle number density, which was shown to be independent of the number of injected particles, was obtained. The resulting ionization equation of state (IEOS) was written in two dimensionless variables. As follows from this IEOS, for two different systems, the ratio of characteristic quantities in corresponding ionization states is the same as that at the critical points (generally, at all singular points). For this reason, one can call such plasmas similar.

The propagation of DAWs is investigated using the fluid approach. Note that the Navier–Stokes equation can be applied for the collective motion of dust particles even at the length scales commensurable with several interparticle distances [38,44,45]. The same approach was used for the strongly coupled Yukawa systems in Ref. [41]. In the fluid dynamics equations, we take into account the electric force and the ion and the neutral drag. Linearization of these equations shows that the balance of forces in an unperturbed medium leads to full compensation of the contribution from the electric field perturbation. Thus, the sound velocity is solely defined by the dust compressibility, which can be calculated on the basis of used IEOS. Here the situation is similar to that for the strongly coupled Yukawa systems [41]. In addition, we allow for the interaction between the particles and the neutrals (neutral drag), which makes it possible to calculate the damping rate of DAWs.

The resulting formula for the dust sound looks quite different from that of Ref. [25] (and also from Ref. [41]). In accordance with IEOS, an increase of the particle number density entails a decrease in the particle charge. Consequently, the dust compressibility and the sound velocity prove to be almost constant everywhere in the bulk of dust cloud, in spite of a considerable variation of the complex plasma parameters. The sound velocity proves to depend weakly on the dust particle radius and gas pressure. For the experiments with argon, it is in a reasonable agreement with the experimental data, in contrast to the calculation using the formula obtained in Ref. [25]. Developed theory makes it possible to perform predictive estimations for conditions typical for the PK-4 experiments.

The paper is organized as follows. In Sec. II we formulate the governing equations for similar complex plasmas. In Sec. III we represent IEOS for the stationary dust cloud in the one-parametric form and explore its singular points, which are the boundaries of characteristic behavior regions of the sound velocity. In Sec. IV we obtain the DAWs' dispersion relation and calculate the sound velocity by derivation of the dust compressibility. We compare the calculation results with available experimental data in Sec. V. The results of this study are summarized in Sec. VI.

II. THE FLUID APPROACH TO COMPLEX PLASMA

Consider a dust cloud in the low-pressure gas discharge. Under microgravity conditions (either in parabolic flights or on board the ISS), a dust particle is subject to three basic forces: the electric driving force, the ion drag force arising from scattering of the streaming ions on dust particles, and the neutral drag force (friction force) due to collisions of the atoms with the moving particles. Note that in a strongly coupled system, the correlation energy originating from particle ordering results in the difference between the volume-averaged electric field and the electric field at the point of particle location. This effect can be included if we introduce the dust pressure. The effect of this pressure on the force balance equation in a stationary plasma is discussed in Sec. III, where we consider the stationary (unperturbed) state of the dust cloud.

If we represent the dust component of complex plasma as a fluid, we have the following basic equations. The first is the Euler equation

$$\frac{\partial \mathbf{v}}{\partial t} + (\mathbf{v}\cdot\nabla)\mathbf{v} + \nu\mathbf{v} = \frac{1}{\rho}(\mathbf{f}_e + \mathbf{f}_{id} - \nabla p), \qquad (1)$$

where $\mathbf{v}(t,\mathbf{r})$ is the velocity field, p and ρ are the pressure and density of a fluid, respectively; $\rho\nu\mathbf{v}$ is the neutral drag force acting on unit volume, $\nu = (8\sqrt{2\pi}/3)\delta m_n n_n v_{T_n} a^2/M$ is the friction coefficient [6,46], $\delta \simeq 1.4$ is the accommodation coefficient; m_n is the mass of a gas molecule; n_n and $v_{T_n} = (T_n/m_n)^{1/2}$ are the number density and thermal velocity of the gas molecules, respectively, $T_n = 300$ K is the temperature of a gas; a is the particle radius, $M = (4\pi/3)\rho_d a^3$ is its mass; ρ_d is the particle material density; and $\mathbf{f}_e$ and $\mathbf{f}_{id}$ are the electric field driving force and the ion drag force acting on unit volume, respectively. Here

$$\mathbf{f}_e = -Zen_d\mathbf{E} = -\frac{aT_e}{e}\Phi n_d\mathbf{E}, \tag{2}$$

where T_e is the electron temperature, $\Phi = -Ze^2/aT_e$ is the dimensionless potential of a dust particle, $\mathbf{E} = (T_e/e)\nabla \ln n_e$ is the electric field strength, n_e is the electron number density, and

$$\mathbf{f}_{id} = \frac{3}{8}\left(\frac{4\pi}{3}\right)^{1/3} n_d^{1/3} n_i \lambda e\mathbf{E}, \tag{3}$$

where λ is the ion mean free path with respect to the collisions against gas atoms, and n_i is the electron number density. Equation (3) is based on a simple estimation of the momentum transfer from the ions to the particle for the case of overlapping Coulomb potentials of neighboring particles [36]. Note that this equation is invalid for an isolated particle.

In addition, the fluid of dust particle obeys the continuity equation

$$\frac{\partial\rho}{\partial t} + \nabla\cdot(\rho\mathbf{v}) = 0. \tag{4}$$

For the dust pressure, we use the expression derived in Ref. [36]

$$p = \frac{1}{8\pi}\left(\frac{a_d T_e}{e\lambda^2}\right)^2 p^*, \quad p^* = \Phi^2 n^{*4/3}, \tag{5}$$

where $n^* = (4\pi/3)\lambda^3 n_d$ and $n_d = \rho/M$ is the particle number density (we mark dimensionless quantities with an asterisk). The expression (5) can be rewritten in the form $p = Z_{\rm th} n_d T_d$, where $Z_{\rm th} = \Gamma/6$ is the compressibility factor for the dust. Since $\Gamma \gg 1$ even for $T_d \gg T_n$, we have $Z_{\rm th} \gg 1$; practically, $Z_{\rm th} > 30$. This agrees qualitatively with the results of calculation for the strongly coupled Yukawa system [47]. Hence, the thermal equation of state for the dust component is fully defined by its strong coupling. Equation (5) results in a typical dust pressure of 10^{-7}–10^{-6} Pa, which is in a good agreement with its estimate following from the assessment of the deformation threshold for a cavity around a large particle in a complex plasma [45] and of the radius of such cavity [36]. The same orders of magnitude of the dust pressure were determined Ref. [39], where the dust acoustic shock waves in strongly coupled dusty plasma were investigated experimentally.

III. SINGULAR POINTS OF IEOS FOR A STATIONARY DUST CLOUD

As follows from Eq. (1), the stationary state condition for a dust cloud ($\mathbf{v} \equiv 0$) is

$$\mathbf{f}_e + \mathbf{f}_{id} - \nabla p = 0. \tag{6}$$

It can be easily shown that the third term on the l.h.s. of Eq. (6) is much smaller than $\mathbf{f}_e$ and $\mathbf{f}_{id}$. Indeed, this term can be represented in the form

$$\nabla p = \frac{dp}{d\rho}\nabla\rho = c^2\nabla\rho = Mn_d c^2 \nabla \ln n_d, \tag{7}$$

where $c^2 = dp/d\rho$. It is shown below that c is defined by ordinary rather than partial derivative and its physical meaning as the sound velocity is clarified in Sec. IV. Since $\mathbf{f}_e = -Zn_d T_e \nabla \ln n_e$, where $|\nabla \ln n_e| \sim 1/L$ and L is the length of the dust cloud, we have $|\mathbf{f}_e| \sim an_d\Phi T_e^2/Le^2$ not too close to the void boundary. Hence, we obtain from Eq. (7) and the estimation $|\nabla \ln n_d| \sim 1/L$ that the condition $|\mathbf{f}_e| \gg |\nabla p|$ is satisfied if

$$\frac{a\Phi T_e^2}{Mc^2e^2} \gg 1. \tag{8}$$

For the conditions of experiment [20], the l.h.s. of (8) is of the order of 10^3 (if $c = 2.4$ cm/s).

Thus, Eq. (6) is reduced to $\mathbf{f}_e + \mathbf{f}_{id} = 0$ or

$$\frac{\pi}{2} r_d^2 n_i \lambda = \frac{aT_e}{e^2}\Phi, \tag{9}$$

which coincides with the balance equation (1) of Ref. [36]. The combination of this equation with the equation for particle potential that follows from the orbital motion limited (OML) approximation [48,49] at $T_e/T_i \gg 1$

$$\theta\Phi e^{\Phi} = \frac{n_e}{n_i}, \tag{10}$$

where $\theta = \sqrt{T_e m_e/T_i m_i}$, $T_i \approx T_n$ and m_i are the ion temperature and mass, respectively, and m_e is the electron mass, and the local quasineutrality condition

$$n_i = \frac{aT_e}{e^2}\Phi n_d + n_e \tag{11}$$

yields the stationary IEOS

$$\theta\Phi e^{\Phi} + \frac{3}{8}\left(\frac{\pi n_i^*}{2\Phi}\right)^{1/2} = 1, \tag{12}$$

where $n_i^* = (e^2\lambda^3/aT_e)n_i$. In contrast to IEOS (1) of Ref. [36], (12) includes a single parameter θ. The solution of Eqs. (9)–(11) can be represented in the form of a one-parametric relation between each desired pair of the variables n_i, n_e, n_d, and Φ (each relation is IEOS as well), e.g., the relation between n_d and Φ. Note that temperatures are included in the parameter θ because they are assumed to be fixed. Thus, for treated system, the dust compressibility is proportional to ordinary rather partial derivative $dp/d\rho$, which implies that differentiation is performed along the ionization equilibrium line.

Figure 1 illustrates two IEOS in the variables n_i^*, n^* and n_i^*, n_e^*, where $n_e^* = (e^2\lambda^3/aT_e)n_e$ is the dimensionless electron number density, for typical conditions of the PK-3

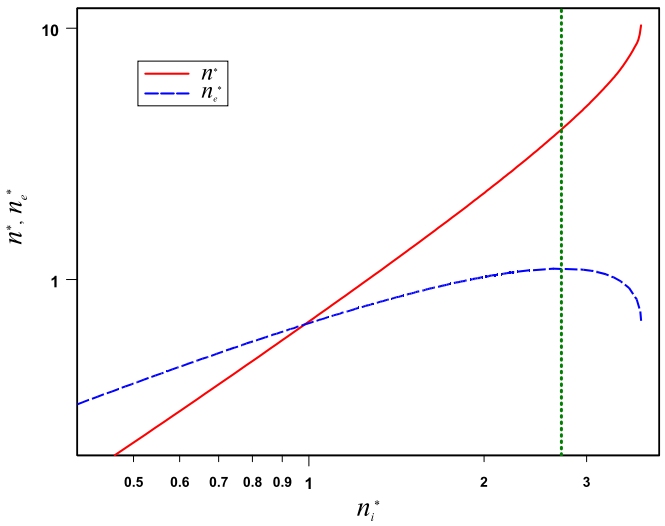

FIG. 1. (Color online) Dimensionless dust particle (n^*, solid line) and electron number density (n_e^*, dashed line) as a function of the dimensionless ion number density n_i^*, $\theta = 0.0431$.

Plus experiment [20]. The dependence $n_e^*(n_i^*)$ shows that both n_i^* and n_e^* have a maximum, which corresponds to two singular points of IEOS. The maximum ion number density n_{ic}^* is reached at the first singular point. Here n^* has a maximum (Fig. 1). The first singular point, which is similar to the critical point and can be associated with the void boundary, is defined by the condition $(dn_i^*/dn_e^*)|_{n_e^*=n_{ec}^*} = 0$. Since $(d\Phi/dn_e^*)|_{n_e^*=n_{ec}^*} \neq 0$, this condition can be rewritten as $(dn_i^*/d\Phi)|_{\Phi=\Phi_c} = 0$ (see Fig. 4 in Ref. [36]). We substitute n_i^* from (12) in the latter derivative to obtain the equation defining the potential Φ_c at the first singular point

$$\theta\Phi_c e^{\Phi_c}(2\Phi_c + 3) = 1. \tag{13}$$

Its solution is

$$\Phi_c \simeq -\ln\theta - \ln\frac{\Phi_0}{2} - \ln(\Phi_0 + 3), \tag{14}$$

where Φ_0 is the potential of an isolated particle obtained from (10) with $n_e = n_i$: $\theta\Phi_0 e^{\Phi_0} = 1$. An approximate solution of this equation is $\Phi_0 \simeq -\ln\theta - \ln(-\ln\theta - 1)$. From (12) and (13) we obtain the ion number density at the first singular point (critical number density)

$$n_{ic}^* = \frac{512}{9\pi}\Phi_c\left(\frac{\Phi_c + 1}{2\Phi_c + 3}\right)^2. \tag{15}$$

Given n_{ic}^*, one can calculate from Eqs. (10)–(12) the dimensionless electron number density n_{ec}^* at the first singular point. With due regard for (13), we obtain

$$n_{ec}^* = \frac{512}{9\pi}\Phi_c\frac{(\Phi_c + 1)^2}{(2\Phi_c + 3)^3}. \tag{16}$$

In a similar way, we obtain from (11) the particle number density at the first singular point

$$n_c^* = \frac{4096}{27}\left(\frac{\Phi_c + 1}{2\Phi_c + 3}\right)^3. \tag{17}$$

Note that n_c^* is the maximum of n^* at fixed θ. At $\theta \to \infty$ and $\Phi_c \to \infty$, $n_c^* \to 512/27$, which is the upper bound for this quantity. The Havnes parameter $H = Zn_d/n_e = (3/4\pi)(\Phi n/n_e^*)$ is introduced to quantify the fraction of negative charge accumulated on the particles. At the first singular point, $H_c = 2(\Phi_c + 1)$.

We exclude n_i from (10) and (12) to derive IEOS in the variables n_e and Φ

$$n_e^* = \frac{128}{9\pi}\theta\Phi^2 e^{\Phi}(1 - \theta\Phi e^{\Phi})^2. \tag{18}$$

The second singular point corresponds to the maximum of n_e (Fig. 1). We denote the quantities corresponding to this point by subscript s. The second singular point is defined by the condition $(dn_e^*/dn_i^*)|_{n_i^*=n_{is}^*} = 0$. Since $(dn_i^*/d\Phi)|_{\Phi=\Phi_s} \neq 0$, we rewrite it in the form $(dn_e^*/d\Phi)|_{\Phi=\Phi_s} = 0$. This yields the equation for the potential Φ_s:

$$\frac{2\theta e^{\Phi_s}(\Phi_s + 1)}{1 - \theta\Phi_s e^{\Phi_s}} = 1 + \frac{2}{\Phi_s}. \tag{19}$$

It is seen from Eq. (19) that $\Phi_s \simeq -\ln 3\theta$ at $\theta \to 0$ and $\Phi_s \simeq 1/2\theta$ at $\theta \to \infty$. The decreasing behavior of $\Phi_s(\theta)$ is illustrated by Fig. 2, in which the solutions of Eq. (19) for different θ are shown.

The combination of (18) and (19) yields the electron number density n_{es}^* at the second singular point

$$n_{es}^* = \frac{512}{9\pi}\Phi_s\frac{(\Phi_s + 2)(\Phi_s + 1)^2}{(3\Phi_s + 4)^3}. \tag{20}$$

One can estimate the ion number density n_{is}^* using (10) and (20),

$$n_{is}^* = \frac{512}{9\pi}\Phi_s\left(\frac{\Phi_s + 1}{3\Phi_s + 4}\right)^2. \tag{21}$$

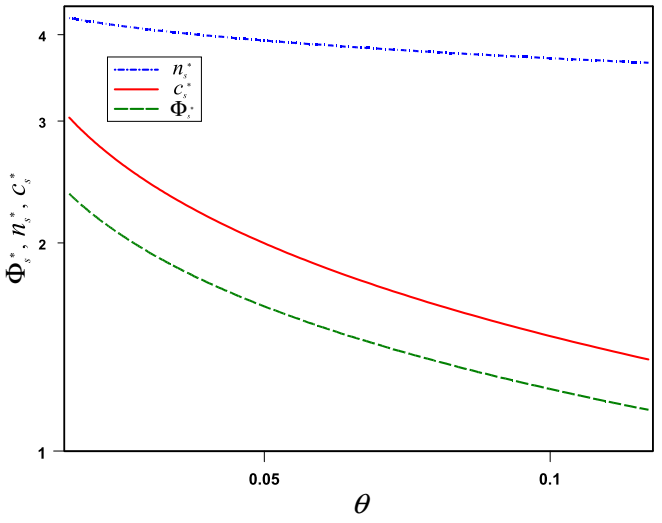

FIG. 2. (Color online) Dimensionless quantities at the second singular point as a function of the temperature parameter θ. Solid line indicates the sound velocity c_s^*; dashed line, the dust particle potential Φ_s^*; and dashed-dotted line, the particle number density n_s^*.

We substitute n_e/n_i from (10) into (11) and then n_i from (11) into (12) to derive IEOS in the variables n^* and Φ:

$$n^* = \frac{512}{27}(1-\theta\Phi e^{\Phi})^3. \tag{22}$$

It follows from (19) and (22) that

$$n_s^* = \frac{4096}{27}\left(\frac{\Phi_s+1}{3\Phi_s+4}\right)^3. \tag{23}$$

It is seen in Fig. 2 that the particle number density at the second singular point $n_s^* \approx 4$, and it is almost independent of θ. At this point, the Havnes parameter is

$$H_s = 2\frac{\Phi_s+1}{\Phi_s+2}. \tag{24}$$

For example, under conditions of the experiment [20], $\theta = 0.0431$, $\Phi_s = 1.708$, and we obtain from (24) $H_s = 1.461$.

Strictly speaking, at the second singular point, the balance equation (9) is invalid along with IEOS (12) and (18) because $\nabla n_e = 0$ and the electric field $\mathbf{E}$ vanishes. However, as follows from (8), the width of singular region is of the same order of magnitude as the interparticle distance. At this point, $\mathbf{E}$ must change its direction. It is possible that this region corresponds to that of inverse ion streaming considered in Ref. [50].

In this section, we have generalized and extended the results of the previous study [36]. We have shown that IEOS for the dust cloud has two singular points, which define the maximum ion and electron number density, respectively, that can be attained in a spatial region occupied by the cloud. The complex plasma parameters at these points are typical for performed experiments. For each singular point, we have obtained analytical expressions for the dimensionless number densities of the electrons, ions, and particles, as well as for the particle electrostatic potential and the Havnes number. We have demonstrated that all these quantities are functions of a single quantity, the dimensionless particle potential Φ at a corresponding point. The latter is defined by the parameter θ, which is a function of the gas molecular mass and the electron temperature.

The spatial location of two singular points can be illustrated in application to the dust cloud in RF discharge plasma (e.g., PK-3 Plus [18] or IMPF-K2 [11] experiments). The configuration of a dust cloud can be very crudely regarded as a sphere with an empty spherical region in the center (void). Then we can associate the first singular point with the void boundary and the second singular point, with a sphere of the radius larger than that of the void. Thus, we have two spatial regions separated by spherical surfaces: the region between the first and the second singular points and the region outside the second singular point.

IV. DUST ACOUSTIC WAVES AND THE SOUND VELOCITY

In what follows, we will treat a nonstationary solution of Eqs. (1) and (4) corresponding to DAWs. As usual, we imply that the wavelength $2\pi c/\omega$, where ω is the frequency, is the largest length scale of the problem and that the wave propagates adiabatically and can be treated in the linear approximation. First, we represent the sum $\mathbf{f}_e + \mathbf{f}_{id}$ in (1) in the form $(g_e + g_{id})\mathbf{E}$, where $g_e = -aT_e\Phi n_d/e$ and $g_{id} = (3/8)(4\pi/3)^{1/3}n_d^{1/3}n_i\lambda e$ [cf. (2) and (3)]. Then we write $g_e = g_{e0} + g_e'$, $g_{id} = g_{id0} + g_{id}'$, and $\mathbf{E} = \mathbf{E}_0 + \mathbf{E}'$, where g_{e0}, g_{id0}, and $\mathbf{E}_0$ are the unperturbed quantities and g_e', g_{id}', and $\mathbf{E}'$, the perturbed ones. Assuming a small perturbation, we write

$$\begin{aligned}\mathbf{f}_e + \mathbf{f}_{id} &\simeq (g_{e0}+g_{id0})\mathbf{E}_0 + (g_{e0}+g_{id0})\mathbf{E}' + (g_e'+g_{id}')\mathbf{E}_0 \\ &= (g_e'+g_{id}')\mathbf{E}_0\end{aligned} \tag{25}$$

due to the force balance condition $g_{e0} + g_{id0} = 0$. It is noteworthy that this condition *cancels out exactly* the field perturbation $\mathbf{E}'$. In other terms, although the field perturbation is nonzero, it does not contribute to the equation of fluid dynamics (1). Therefore, the effect of charge separation due to the ion shift that determines the sound velocity in equilibrium plasma [25] is fully compensated in the complex plasma of gas discharge treated in this work. Thus, the sound velocity is solely defined by the dust compressibility. A similar situation takes place in strongly coupled Yukawa systems [41].

Calculation of the sum $g_e' + g_{id}'$ in (25) is a separate problem, which cannot be solved within the framework of the model [36] we use in this work. In fact, the model assumes that at least one stationary spatial distribution of the number densities of the charged components (electrons, ions, and particles) is known. Hence, to evaluate $g_e' + g_{id}'$, we have either to develop a self-consistent theory of the complex discharge plasma (which is now lacking) or to add another assumption to our model, in other words, to redefine the model so that it would be applicable for dynamic processes. Note that the models of equilibrium plasma and of strongly coupled Yukawa systems are also defined by a set of assumptions. Our additional assumption will be $g_e' = -g_{id}'$, which means simply that the variations of all quantities in the sound wave are related by IEOS (12) or that the electric and ion drag forces are always kept in balance. This assumption is similar to that made for an ordinary acoustic wave. What is more important, this assumption allows one to provide an interpretation of the sound velocity isotropy known from experiment. Indeed, the sound velocity was found to be independent of the wave propagation direction with respect to the direction of external electric field $\mathbf{E}_0$, which is almost radial in some setups. If only $g_e' \neq -g_{id}'$, the resulting sound velocity would be anisotropic.

With this assumption, Eq. (1) is reduced to

$$\frac{\partial \mathbf{v}}{\partial t} + (\mathbf{v}\cdot\nabla)\mathbf{v} + \nu\mathbf{v} = -\frac{1}{\rho}\nabla p. \tag{26}$$

Actually, (26) corresponds to a fluid of soft spheres with no Coulomb interaction. This equation was successfully applied for the problem of dust particle collective dynamics [38,44,45]. Equation (26) differs from the standard wave equation by the neutral drag force term on its l.h.s. We linearize Eqs. (26) and (4) following the common procedure [51] by substitution of $p = p_0 + p'$ and $\rho = \rho_0 + \rho'$, where p_0 and ρ_0 are the stationary (unperturbed) pressure and density of the dust particles and p' and ρ' are their perturbations, respectively. With due regard for the fact that $p' = c^2\rho'$, we obtain

$$\frac{1}{c^2}\frac{\partial p'}{\partial t} + \rho_0\nabla\cdot\mathbf{v} = 0 \tag{27}$$

and

$$\frac{\partial \mathbf{v}}{\partial t} + \nu \mathbf{v} = -\frac{\nabla p'}{\rho_0}. \tag{28}$$

We represent the velocity in the form $\mathbf{v} = \nabla\psi$ to derive from (28)

$$p' = -\rho_0\left(\frac{\partial \psi}{\partial t} + \nu\psi\right). \tag{29}$$

Substitution of (29) into (27) yields the wave equation

$$\frac{\partial^2 \psi}{\partial t^2} + \nu\frac{\partial \psi}{\partial t} = c^2\Delta\psi, \tag{30}$$

where c is the sound velocity. If the sought solution has the form $\psi = Ae^{i(\omega t - \mathbf{k}\cdot\mathbf{r})}$, where $\mathbf{k}$ is the wave vector, then we arrive at the dispersion relation $c^2k^2 = \omega^2 - i\omega\nu$ or

$$\frac{ck}{\omega} = \frac{\sqrt{\sqrt{1+\tilde{\nu}^2}+1}}{\sqrt{2}} - i\frac{\sqrt{\sqrt{1+\tilde{\nu}^2}-1}}{\sqrt{2}}, \tag{31}$$

where $\tilde{\nu} = \nu/\omega$. If $\tilde{\nu} \ll 1$ then

$$\frac{ck}{\omega} \simeq 1 + \frac{\tilde{\nu}^2}{8} - i\frac{\tilde{\nu}}{2}. \tag{32}$$

It is seen from (32) that the sound velocity is not much different from c, and the damping length $c\nu/2$ is defined by a half of the damping frequency ν.

One can calculate c by differentiation of (5) with respect to $\rho = Mn_d$,

$$\frac{dp^*}{dn^*} = 2\Phi n^{*4/3}\left(\frac{dn^*}{d\Phi}\right)^{-1} + \frac{4}{3}\Phi^2 n^{*1/3}. \tag{33}$$

We differentiate n^* with due regard for (22),

$$\frac{dn^*}{d\Phi} = -8\theta n^{*2/3}e^{\Phi}(1+\Phi), \tag{34}$$

to arrive at

$$c = \frac{aT_e c^*}{e\sqrt{6M\lambda}},$$
$$c^{*2} = \frac{4}{3}\Phi^2 n^{*1/3}\left[1 - \frac{3}{2}\frac{n^{*1/3}}{(\Phi+1)(8-3n^{*1/3})}\right], \tag{35}$$

where $n^{*1/3} = (8/3)(1-\theta\Phi e^{\Phi})$. Note that the sound velocity (along with the particle compressibility) is a continuous function at the second singular point.

Using (13) and (35) one can easily show that $c^2(\Phi_c) = 0$, $c^2 > 0$ at $\Phi > \Phi_c$, and $c^2 < 0$ at $\Phi < \Phi_c$. Since $n^*(\Phi)$ is a decreasing function, in the latter case $n > n_c$. We can conclude that the corresponding branch of solutions of Eq. (12) relates to an *unstable* state of the dust cloud with a negative compressibility. Such a state would tend to collapse and to quench the discharge. Hence, we confine ourselves to the treatment of a positive compressibility branch with $\Phi > \Phi_c$ and $n < n_c$.

According to (35) the sound velocity is a function of the spatial coordinate. This dependence can be qualitatively illustrated if we consider the dependence $c(n_i)$ determined by (12) and (35) (Fig. 3). For Fig. 3, the experimental conditions [20] were selected as typical ones. It is seen that the sound velocity is almost independent of the ion number density,

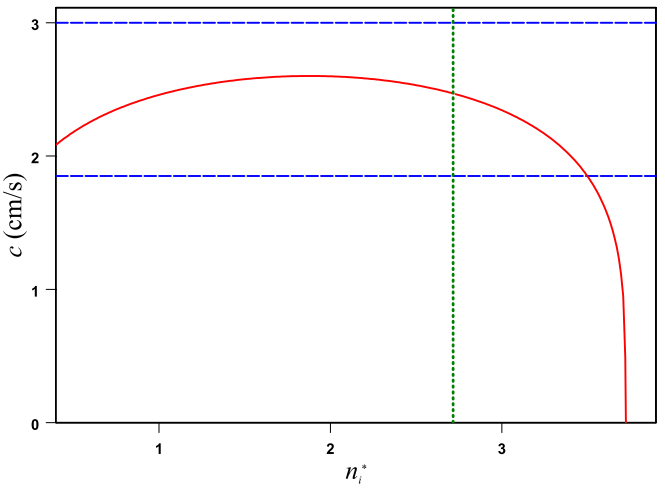

FIG. 3. (Color online) Dependence of the sound velocity on the dimensionless ion number density (solid line), $\theta = 0.0431$. Dashed lines indicate the boundaries of a band, in which the sound velocity measured at different locations inside the dust cloud are scattered [20], and dotted line points to the location of the second singular point.

i.e., of the coordinate in the volume of the dust cloud. This is accounted for by the fact that the particle pressure (5) increases but the particle potential decreases with the increase of the dust number density. The increase in n^* is almost compensated by the decrease in Φ. Thus, $c(n_i)$ has a very wide maximum with the maximum point situated approximately in the center of a cloud (Fig. 3). The variation of $c(n_i)$ is so small that the entire curve lies within the band, in which the sound velocity measured at different locations inside the dust cloud is scattered [20]. This accounts for the fact that the dependence of sound velocity on the coordinate was not resolved in experiments. It is also seen in Fig. 3 that in the close vicinity of the inner boundary of the cloud, which we associate with the first singular point, c vanishes very sharply. Apparently, behavior of c in this region cannot be resolved experimentally as well.

Obviously, the average sound velocity is close to its value at the second singular point c_s. Using (19) and (23) we obtain from (35)

$$c_s = \frac{Zec_s^*}{\sqrt{6M\lambda}} = \frac{T_e c_s^*}{e\sqrt{8\pi\rho_d a\lambda}}, \quad c_s^* = \frac{8}{3}\frac{\Phi_s(\Phi_s+1)}{\sqrt{(3\Phi_s+4)(\Phi_s+2)}}. \tag{36}$$

It is seen in Fig. 2 that c_s^* is a decreasing function of the temperature parameter θ. Since $\Phi_s \to \infty$ at $\theta \to 0$ (Sec. III), $c_s \to \infty$ in this limit; at $\theta \to \infty$, we have $\Phi_s \to 0$ and $c_s \to 0$. As it follows from (36), c_s is weakly dependent on the particle radius a.

V. ANALYSIS OF EXPERIMENTAL DATA

In Fig. 4 we compare the calculation using formula (36) with the available results of experiments where the sound velocity was determined. In these experiments performed under microgravity conditions both in parabolic flights and on board the ISS, a 3D dust cloud was formed in argon RF

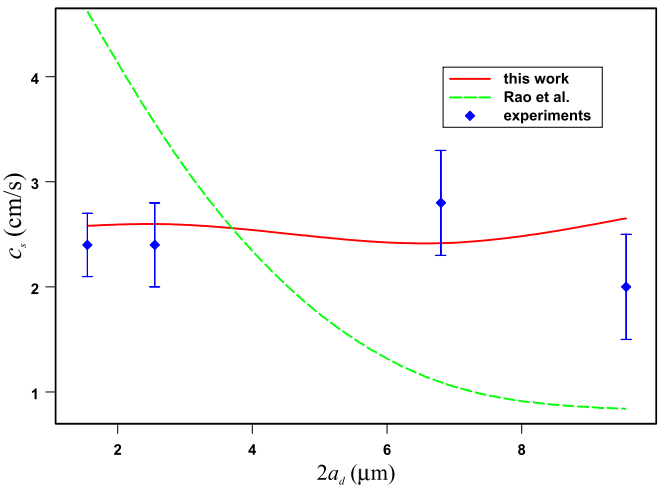

FIG. 4. (Color online) Sound velocity in the dust clouds formed by the particles of different diameter in argon RF discharge. Solid line indicates the calculation using (36); dashed line, using the formula in Ref. [25] (37). Dots represent experimental data for different particle diameter (from left to right): $2a_d = 1.55$ [19], 2.55 [20], 6.8 [11,12], and 9.55 μm [11,14].

discharge. One can confirm a satisfactory agreement between proposed theory and experiment in a wide range of the particle diameter. Note a very weak dependence of c_s on this parameter. According to (36), this follows not only from the dependence $c_s \sim 1/\sqrt{a}$ but also from $c_s \sim 1/\sqrt{\lambda}$ and from the fact that the experimental pressure is higher for larger particles. A good correlation between (36) and experiment is illustrated by Fig. 3, where the range of n_i^* variation corresponds to the experiment [20] (for the spatial distributions of n_i and n_d in the dust cloud; see Ref. [36]). The variation of sound velocity is noticeably smaller than the experimental data scatter.

Figure 4 also shows the results of calculation using the formula $c = \sqrt{ZT_i H/M(H+1)}$ [25]. For the correctness of comparison, we estimate c at the second singular point. Thereby, we include the effect of particle charge decrease as compared to the charge of an isolated particle, which is sometimes called "the charge cannibalism" [52,53]. Using (24) we obtain for this point

$$c_s = \frac{1}{ae}\sqrt{\frac{3T_eT_i}{2\pi\rho_d}\frac{\Phi_s^2}{3\Phi_s+4}}. \qquad (37)$$

Note that (37) is entirely different from (36). Figure 4 shows that formula (37) demonstrates a trend incompatible with that of experimental data. Estimates show a significant variation of the sound velocity [25] as a function of the position in the dust cloud. Under conditions of Ref. [20], c would change by a factor of 1.6, which could be detected in this experiment. Thus, one can confirm a better overall applicability of formula (35).

Although the linear theory of DAWs is not applicable to the self-excited nonlinear dust-density waves, it is of interest to consider their phase velocities determined in experiments [54,55]. In the experiment [54] performed in argon with particles of diameter 9.55 μm under microgravity conditions, the phase velocity varied in the range from 1 to 3 cm/s. In the ground-based experiment [55], the particles of the diameter

TABLE I. Parameters of a dust cloud in the PK-4 experiments with neon complex plasma for the different diameters $2a$ of monodisperse particles and their number density n_d (experimental data were borrowed from Ref. [22]). The "dust invariant" $\kappa = r_d^2/aT_e$ and the sound velocity c_s (36) at different neon pressures were calculated at $T_e = 7$ eV for the silica particles of $2a = 1.2$ μm and the melamine formaldehyde particles of larger diameters.

$2a$, μm	n_d, 10^4 cm^{-3}	κ, cm/eV	c_s, cm/s ($p_n = 15$ Pa)	c_s, cm/s ($p_n = 30$ Pa)
1.2	20	0.268	4.14	5.85
6.8	4	0.138	1.95	2.76
11	1.3	0.181	1.53	2.17

0.97 μm in argon were used, and the average phase velocity was found to be 7.5 cm/s. In both studies, the phase velocity showed considerable spatial variations. These results are best fitted by Eq. (37) (cf. dashed line in Fig. 4). Apparently, a qualitative difference from the results concerning the sound velocity can be explained by the fact that the phase velocity of dust-density waves is defined by the ion density modulation, which is explicitly taken into account in (37) but does not contribute to the sound velocity in our case.

In the ongoing PK-4 experiments, dust clouds are predominantly formed in the dc (or combined dc+RF) discharge in neon. First, it is necessary to check if IEOS used in this work is applicable for such systems. The results of calculation of the "dust invariant" $\kappa = r_d^2/aT_e$, which was introduced in Ref. [36] for the argon RF discharge, for conditions of the PK-4 experiment with neon is presented in Table I. It is seen that κ is not much different for neon and argon ($\kappa = 0.209$ cm/eV [36]). This makes it possible to apply formula (36) for the prediction of typical sound velocities in the PK-4 experiments. It is worth mentioning that for $2a = 1.2$ μm, κ is twice as high as for 6.8 μm (Table I). This may indicate a poor applicability of the approximation of similar complex plasmas for the smallest particles ($2a < 2$ μm). The reason why the theory may be flawed in this range of diameters may lie in the fact that for the smallest particles, the Debye length and the momentum transfer cross section for an isolated particle are no longer greater than r_d, so that the Coulomb potentials of neighboring particles do not overlap [36]. Therefore, the momentum transfer cross section of the ion scattering on particles may be different from that used in this work. Another one reason may be the higher electron temperature as compared to argon at low neon pressure. Under such conditions, the ion drag force can be proportional to the square of the electric field, which is not taken into account in used formula for the ion drag force (3).

One can also suggest the mechanisms of particle charging other than OML approximation, which can effectively change θ, such as the ion-neutral collisions [21,56]. However, as was demonstrated in Refs. [21,56], the effect of collisions, which reduces the particle charge, is negligibly small at the pressures $p_n < 30$ Pa and the Havnes number greater than unity. It is noteworthy that the typical particle charge $Z = -aT_e\Phi_c/e^2$ calculated using formula (14) for $T_e = 7$ eV and $a = 1.3$ μm amounts to $|Z| \approx 3500$, which is almost half the charge of

an isolated particle. This estimate is close to the charge determined in experiment [21] performed at the same electron temperature and particle radius. Note that a particle flow rather than a stationary dust cloud was realized in Ref. [21], for which (14) is not directly applicable. We also note that DAWs are unlikely to be resolved at $p_n > 30$ Pa due to the high damping rate [35], so that inclusion of the effect of ion-neutral collisions would not change the numerical results significantly.

Thus, in PK-4 experiments, one can expect the sound velocity ranging from 2 to 3 cm/s with a weak trend to the increase with the increase in pressure and the decrease in particle diameter, while greater velocities seem to be overestimated in Table I. It is worth mentioning that for neon, formula (37) would lead to the sound velocities ranging from 0.89 to 7.33 cm/s.

Unfortunately, no direct measurement of the sound velocity was performed in PK-4 experiments. However, the experimental data on dust acoustic shock waves are best fitted at a sound velocity of 2.5 cm/s [39]. For melamine formaldehyde particles of diameter $2a = 3.4$ μm used in this experiment, $p_n = 15$ Pa, and $T_e = 7$ eV, formula (36) yields a close value $c_s = 2.76$ cm/s.

The sound velocity was measured for the RF discharge in neon in the PK-3 Plus experiment [35]. For the silica particles of the diameter $2a = 1.55$ μm, the neon pressure $p_n = 15$ Pa, and the electron temperature $T_e = 7$ eV ($\theta = 0.0858$), the sound velocity reported in Ref. [35] is $c_s = 0.96$ cm/s. For this set of parameters, formula (36) yields $c_s = 3.6$ cm/s and (37), $c_s = 5.7$ cm/s. Despite that the result of (36) is significantly closer to the experiment, it is still rather inappropriate. To find the reason of such discrepancy, we will analyze the basic limits of validity of IEOS formulated in Ref. [36]. The Coulomb momentum transfer cross section for an isolated particle $\sim(aT_e/T_i\Phi)^2$ must be much greater than the cross section of the particle Wigner-Seitz cell $\sim r_d^2$. At the second singular point, we have from (23) $r_d \approx 0.63\lambda$, and this condition can be written as

$$2.5\left(\frac{a\Phi_s T_e}{\lambda T_i}\right)^2 \gg 1. \tag{38}$$

The second condition requires that the maximum impact parameter of ion scattering on an isolated particle with due regard for the Debye screening $(2\Phi a\lambda_D T_e/T_i)^{1/2}$, where $\lambda_D = (T_i/4\pi n_i e^2)^{1/2}$ is the ion Debye screening length, is much larger than r_d. At the second singular point, we use (21) and (23) to write this condition as

$$0.33\Phi_s^{1/2}\frac{3\Phi_s+4}{\Phi_s+1}\left(\frac{aT_e}{\lambda T_i}\right)^{1/2} \gg 1. \tag{39}$$

As is seen from (38) and (39), the limit of validity of used theory is reached at sufficiently small particle diameters. Under the experimental conditions [35], the l.h.s. of (38) and (39) are close to unity, and therefore, the theory may be flawed in this region.

In addition to the reasons of the inapplicability of (36) for the smallest particles discussed above, one can assume that in the presence of the particles in RF discharge, the electron temperature can be lower than that in the absence of the particles, i.e., less than 7 eV. However, for the experiment [35], there is a good agreement between the damping rates of DAWs first measured for a 3D dust cloud and the theoretical result $\nu/2$ [see (32)]. In fact, for $p_n = 20$ Pa, the damping rates are 43 and 46 s^{-1} from the theory and experiment, respectively, and for $p_n = 15$ Pa, 33 and 32 s^{-1}.

VI. CONCLUSION

To summarize, we have calculated the sound velocity corresponding to DAWs in a nonequilibrium stationary 3D dust cloud formed in the low pressure ac-dc discharge under microgravity conditions. The dust cloud is assumed to conform to the model of similar complex plasmas, which treats a stationary state of the dust cloud as a balance between the electric force from an external electric field of the discharge and the ion drag force. The ionization state of such a system is fully defined by the one-parametric IEOS, which can relate each pair of four dimensionless variables. To find characteristic regions of behavior of the sound velocity, we determine two singular points of this IEOS related to the maximum of the ion and electron number densities, respectively. We use the fluid approach (the Euler and continuity equations) to account for the dynamics of the dust plasma component. We have demonstrated that in the presence of the external electric field, the field perturbation associated with the sound wave is dominated by the gradient of the dust pressure, which emerges due to the particle correlations in a strongly coupled system. Thus, the sound velocity is fully determined by the compressibility of the dust cloud. We have shown that only one branch of two IEOS solutions that implies the high particle potentials and low number densities can be realized. We have included the neutral drag term in the Euler equation to derive a dispersion relation that makes it possible to estimate the damping rate of a sound wave. Based on this equation, we calculated the dependence of the sound velocity on the ion number density, which mimics a real spatial distribution of this quantity in the dust cloud. The sound velocity was found to be almost independent of the coordinate and to assume its typical value at the second singular point.

Comparison with available experimental data reveals a good correspondence with the measurements of sound velocity. The obtained formula for this quantity can account for all experimentally observed regularities, such as independence of the coordinate, of the particle radius, and of the gas pressure. The damping rates of a dust cloud in neon are also in good agreement with experiment.

A comparison with the well-known result of Ref. [25] performed at the same point of the plasma ionization state diagram, thus including the effect of particle charge lowering, shows a trend entirely different from experimentally observed one. For small particle diameters, the calculated sound velocity is more than twice as high as the experimental one, and for large diameters, vice versa. This is not surprising because the result [25] is quite correct for equilibrium ideal plasma in the absence of an external electric field. In contrast, our system is strongly nonequilibrium and strongly coupled.

In regard to the PK-4 experiment, the analyses of up-to-date data demonstrates that the dust cloud in neon can be quantified by the "dust invariant" of our model, which have approximately the same value for different dust clouds in neon.

Its value is close to that typical for PK-3 Plus experiments. This allows one to make some predictive estimations of the sound velocity, which can be helpful in the analysis of dust acoustic shock wave propagation. A best fit sound velocity that follows from such analysis [39] almost coincides with that calculated in this work.

A single experimental datum, which proved to be incompatible with the proposed theory, is a low sound velocity in the PK-3 Plus experiment with neon [35], which is more than twice as low as the theoretical estimation. We show that our theory is valid for sufficiently large particles, but the dust particles used in the experiment [35] are too small for the theory. A correct approach to the theory of a cloud of small particles requires treatment of the Yukawa rather than the Coulomb system, although the corresponding model may not have the property of similarity. Another problem of interest is the sound propagation in a cloud with different particle sizes. These problems will be addressed in the future.

ACKNOWLEDGMENT

This research is supported by the Russian Science Foundation Grant No. 14-50-00124.

[1] V. E. Fortov and G. E. Morfill, eds., *Complex and Dusty Plasmas: From Laboratory to Space*, Series in Plasma Physics (CRC Press, Boca Raton, FL, 2009).
[2] J. H. Chu and Lin I, Phys. Rev. Lett. **72**, 4009 (1994).
[3] H. Thomas, G. E. Morfill, V. Demmel, J. Goree, B. Feuerbacher, and D. Möhlmann, Phys. Rev. Lett. **73**, 652 (1994).
[4] Y. Hayashi and S. Tashibana, Jpn. J. Appl. Phys. **33**, L804 (1994).
[5] S. V. Vladimirov, K. Ostrikov, and A. A. Samarian, *Physics and Applications of Complex Plasmas* (Imperial College, London, 2005).
[6] V. Fortov, A. Ivlev, S. Khrapak, A. Khrapak, and G. Morfill, Phys. Rep. **421**, 1 (2005).
[7] P. K. Shukla and B. Eliasson, Rev. Mod. Phys. **81**, 25 (2009).
[8] M. Bonitz, C. Henning, and D. Block, Rep. Prog. Phys. **73**, 066501 (2010).
[9] D. I. Zhukhovitskii, O. F. Petrov, T. W. Hyde, G. Herdrich, R. Laufer, M. Dropmann, and L. Matthews, New J. Phys. **17**, 053041 (2015).
[10] G. E. Morfill, U. Konopka, M. Kretschmer, M. Rubin-Zuzic, H. M. Thomas, S. K. Zhdanov, and V. Tsytovich, New J. Phys. **8**, 7 (2006).
[11] D. Caliebe, O. Arp, and A. Piel, Phys. Plasmas **18**, 073702 (2011).
[12] A. Piel, O. Arp, M. Klindworth, and A. Melzer, Phys. Rev. E **77**, 026407 (2008).
[13] K. O. Menzel, O. Arp, and A. Piel, Phys. Rev. E **83**, 016402 (2011).
[14] O. Arp, D. Caliebe, and A. Piel, Phys. Rev. E **83**, 066404 (2011).
[15] M. Schwabe, S. K. Zhdanov, H. M. Thomas, A. V. Ivlev, M. Rubin-Zuzic, G. E. Morfill, V. I. Molotkov, A. M. Lipaev, V. E. Fortov, and T. Reiter, New J. Phys. **10**, 033037 (2008).
[16] G. E. Morfill, H. M. Thomas, U. Konopka, H. Rothermel, M. Zuzic, A. Ivlev, and J. Goree, Phys. Rev. Lett. **83**, 1598 (1999).
[17] S. A. Khrapak, B. A. Klumov, P. Huber, V. I. Molotkov, A. M. Lipaev, V. N. Naumkin, H. M. Thomas, A. V. Ivlev, G. E. Morfill, O. F. Petrov, V. E. Fortov, Yu. Malentschenko, and S. Volkov, Phys. Rev. Lett. **106**, 205001 (2011).
[18] H. M. Thomas, G. E. Morfill, V. E. Fortov, A. V. Ivlev, V. I. Molotkov, A. M. Lipaev, T. Hagl, H. Rothermel, S. A. Khrapak, R. K. Suetterlin, M. Rubin-Zuzic, O. F. Petrov, V. I. Tokarev, and S. K. Krikalev, New J. Phys. **10**, 033036 (2008).
[19] K. Jiang, V. Nosenko, Y. F. Li, M. Schwabe, U. Konopka, A. V. Ivlev, V. E. Fortov, V. I. Molotkov, A. M. Lipaev, O. F. Petrov, M. V. Turin, H. M. Thomas, and G. E. Morfill, Europhys. Lett. **85**, 45002 (2009).
[20] M. Schwabe, K. Jiang, S. Zhdanov, T. Hagl, P. Huber, A. V. Ivlev, A. M. Lipaev, V. I. Molotkov, V. N. Naumkin, K. R. Sütterlin, H. M. Thomas, V. E. Fortov, G. E. Morfill, A. Skvortsov, and S. Volkov, Europhys. Lett. **96**, 55001 (2011).
[21] S. A. Khrapak, S. V. Ratynskaia, A. V. Zobnin, A. D. Usachev, V. V. Yaroshenko, M. H. Thoma, M. Kretschmer, H. Höfner, G. E. Morfill, O. F. Petrov, and V. E. Fortov, Phys. Rev. E **72**, 016406 (2005).
[22] V. Fortov, G. Morfill, O. Petrov, M. Thoma, A. Usachev, H. Hoefner, A. Zobnin, M. Kretschmer, S. Ratynskaia, M. Fink, K. Tarantik, Yu. Gerasimov, and V. Esenkov, Plasma Phys. Control. Fusion **47**, B537 (2005).
[23] M. A. Fink, M. H. Thoma, and G. E. Morfill, Microgravity Sci. Technol. **23**, 169 (2011).
[24] A. V. Zobnin, A. D. Usachev, O. F. Petrov, and V. E. Fortov, Phys. Plasmas **21**, 113503 (2014).
[25] N. N. Rao, P. K. Shukla, and M. Y. Yu, Planet. Space Sci. **38**, 543 (1990).
[26] R. L. Merlino, J. Plasma Phys. **80**, 773 (2014).
[27] O. Havnes, F. Li, F. Melandsø, T. Aslaksen, T. W. Hartquist, G. E. Morfill, T. Nitter, and V. Tsytovich, J. Vac. Sci. Technol. A **14**, 525 (1996).
[28] D. Samsonov, J. Goree, Z. W. Ma, A. Bhattacharjee, H. M. Thomas, and G. E. Morfill, Phys. Rev. Lett. **83**, 3649 (1999).
[29] D. Samsonov, J. Goree, H. M. Thomas, and G. E. Morfill, Phys. Rev. E **61**, 5557 (2000).
[30] A. Melzer, S. Nunomura, D. Samsonov, Z. W. Ma, and J. Goree, Phys. Rev. E **62**, 4162 (2000).
[31] V. Nosenko, J. Goree, Z. W. Ma, and A. Piel, Phys. Rev. Lett. **88**, 135001 (2002).
[32] V. Nosenko, J. Goree, Z. W. Ma, D. H. E. Dubin, and A. Piel, Phys. Rev. E **68**, 056409 (2003).
[33] S. K. Zhdanov, D. Samsonov, and G. E. Morfill, Phys. Rev. E **66**, 026411 (2002).
[34] S. K. Zhdanov, G. E. Morfill, D. Samsonov, M. Zuzic, and O. Havnes, Phys. Rev. E **69**, 026407 (2004).
[35] D. I. Zhukhovitskii, V. E. Fortov, V. I. Molotkov, A. M. Lipaev, V. N. Naumkin, H. M. Thomas, A. V. Ivlev, M. Schwabe, and G. E. Morfill, Phys. Plasmas **22**, 023701 (2015).
[36] D. I. Zhukhovitskii, V. I. Molotkov, and V. E. Fortov, Phys. Plasmas **21**, 063701 (2014).

[37] L. D. Landau and E. M. Lifshitz, *Statistical Physics* (Elsevier, Oxford, 1980).
[38] D. I. Zhukhovitskii, V. E. Fortov, V. I. Molotkov, A. M. Lipaev, V. N. Naumkin, H. M. Thomas, A. V. Ivlev, M. Schwabe, and G. E. Morfill, Phys. Rev. E **86**, 016401 (2012).
[39] A. Usachev, A. Zobnin, O. Petrov, V. Fortov, M. H. Thoma, H. Höfner, M. Fink, A. Ivlev, and G. Morfill, New J. Phys. **16**, 053028 (2014).
[40] E. A. Lisin, I. I. Lisina, O. S. Vaulina, and O. F. Petrov, Phys. Plasmas **22**, 033704 (2015).
[41] S. A. Khrapak and H. M. Thomas, Phys. Rev. E **91**, 033110 (2015).
[42] S. A. Khrapak, A. G. Khrapak, A. V. Ivlev, and H. M. Thomas, Phys. Plasmas **21**, 123705 (2014).
[43] S. A. Khrapak and A. G. Khrapak, Phys. Plasmas **21**, 104505 (2014).
[44] A. V. Ivlev and D. I. Zhukhovitskii, Phys. Plasmas **19**, 093703 (2012).
[45] D. I. Zhukhovitskii, A. V. Ivlev, V. E. Fortov, and G. E. Morfill, Phys. Rev. E **87**, 063108 (2013).
[46] P. Epstein, Phys. Rev. **23**, 710 (1924).
[47] S. A. Khrapak, N. P. Kryuchkov, S. O. Yurchenko, and H. M. Thomas, J. Chem. Phys. **142**, 194903 (2015).
[48] H. M. Mott-Smith and I. Langmuir, Phys. Rev. **28**, 727 (1926).
[49] J. E. Allen, Phys. Scr. **45**, 497 (1992).
[50] G. Gozadinos, A. V. Ivlev, and J. P. Boeuf, New J. Phys. **5**, 32 (2003).
[51] L. D. Landau and E. M. Lifshitz, *Fluid Mechanics* (Pergamon Press, New York, 1959).
[52] A. Barkan, N. D'Angelo, and R. L. Merlino, Phys. Rev. Lett. **73**, 3093 (1994).
[53] S. A. Khrapak, H. M. Thomas, and G. E. Morfill, Europhys. Lett. **91**, 25001 (2010).
[54] K. O. Menzel, O. Arp, and A. Piel, Phys. Rev. Lett. **104**, 235002 (2010).
[55] I. Pilch, T. Reichstein, and A. Piel, Phys. Plasmas **16**, 123709 (2009).
[56] S. A. Khrapak, B. A. Klumov, P. Huber, V. I. Molotkov, A. M. Lipaev, V. N. Naumkin, A. V. Ivlev, H. M. Thomas, M. Schwabe, G. E. Morfill, O. F. Petrov, V. E. Fortov, Y. Malentschenko, and S. Volkov, Phys. Rev. E **85**, 066407 (2012).